Hindawi Publishing Corporation
Journal of Nanomaterials
Volume 2012, Article ID 642080, 10 pages
doi:10.1155/2012/642080

Research Article

Electrically Conductive Compounds of Polycarbonate, Liquid Crystalline Polymer, and Multiwalled Carbon Nanotubes

Penwisa Pisitsak,[1,2] Rathanawan Magaraphan,[1] and Sadhan C. Jana[3]

[1] *Polymer Processing and Polymer Nanomaterials Research Unit, The Petroleum and Petrochemical College, Chulalongkorn University, Bangkok 10330, Thailand*
[2] *Department of Textile Science and Technology, Faculty of Science and Technology, Thammasat University, Rangsit Center, Pathum Thani 12121, Thailand*
[3] *Department of Polymer Engineering, University of Akron, Akron, OH 44325-0301, USA*

Correspondence should be addressed to Rathanawan Magaraphan, rathanawan.k@chula.ac.th

Received 24 April 2012; Revised 12 July 2012; Accepted 29 July 2012

Academic Editor: Suprakas Sinha Ray

A thermotropic liquid crystalline polymer (LCP) was blended with polycarbonate (PC) and multiwalled carbon nanotube (CNT) with the goal of improving electrical conductivity and mechanical properties over PC. The LCP was anticipated to produce fibrillar domains in PC and help improve the mechanical properties. The study was carried out using two grades of LCP—Vectra A950 (VA950) and Vectra V400P (V400P). The compounds contained 20 wt% LCP and 0.5 to 15 wt% CNT. The compounds were prepared by melt-blending in a twin-screw minicompounder and then injection molded using a mini-injection molder. The fibrillar domains of LCP were found only in the case of PC/VA950 blend. However, these fibrils turned into droplets in the presence of CNT. It was found that CNT preferentially remained inside the LCP domains as predicted from the value of spreading coefficient. The electrical conductivity showed the following order with the numbers in parenthesis representing the electrical percolation threshold of the compounds: PC/CNT (1%) > PC/VA950P/CNT (1%) > PC/V400P/CNT (3%). The storage modulus showed improvements with the addition of CNT and VA950.

1. Introduction

Over the last two decades, blends of thermoplastic polymers with liquid crystalline polymer (LCP) received considerable interests from both academic and industrial researchers. The dispersed LCP domains tend to elongate during melt processing and subsequently form aligned fibrils capable of reinforcing the matrix polymer. The aligned fibril formation in these *in situ composites* greatly depended on the choice of polymer matrix and the selection of proper processing conditions. The droplets, short fibrils, networks of droplets and fibrils, and continuous fibrous LCP structures in thermoplastic polymers have been reported [1–7]. The research on *in situ* composites mainly dealt with unique morphology and consequent enhancement of mechanical properties, while those addressing the electrical properties are limited [8–10]. In this context, introduction of carbon nanotubes (CNTs) in thermoplastic polymer/LCP blends can offer additional improvements in mechanical properties in addition to offering excellent electrical and thermal conductivity. However, high cost and limited availability of CNTs often serve as deterrent to development of more widespread applications of composites containing CNTs. In this study, CNTs were introduced in blends of polycarbonate (PC) and LCP with the aim of obtaining synergistic effects, such as strong mechanical properties from fibrillar LCP domains and electrical conductivity from CNTs. The interplay of CNTs with the morphology of PC/LCP blends or the possibility of selective localization of CNTs in PC or LCP was not known a priori. A summary of existing literature on electrically conductive immiscible blends, especially those of carbon black, carbon nanofibers (CNFs), and CNTs is presented below.

Immiscible polymer blend systems have been effectively used in the production of electrically conductive composites via preferential localization of the conductive fillers, for example, carbon black, in one of the phases [11–14]. This gives rise to double percolation—whereby electrically conductive percolation networks develop in one of the cocontinuous phases. This phenomenon was mostly observed for blends with close to 50 : 50 weight ratios of the component polymers. Dharaiya and coworkers recently exploited chaotic mixing conditions to produce fibrillar morphology of polypropylene (PP) in blending of 90 parts by weight of polyamide 6 (PA6) with 10 parts by weight of PP and used the cocontinuous fibrils of PP to obtain electrically conductive PP/PA6 compounds at only 1 wt% conductive grade carbon black [15].

Other researchers also exploited the preferential localization concept in immiscible blends filled with carbon nanofibers [16, 17], or CNTs [18–21], and reported success in terms of much reduced electrical percolation threshold compared to individual polymer compounds. A schematic representation of the double percolation phenomenon in involving CNTs is shown in Figure 1. Pötschke et al. [18, 19] studied electrical conductivity of polycarbonate (PC)/polyethylene blends filled with CNTs and claimed that CNT connected the two polymer phases. The resulting composites showed electrical percolation threshold at 0.41 vol.% CNT. Pötschke et al. [20] used metallocene-based complex for *in-situ* polymerization of ethylene directly from the CNT surface which resulted in good filler dispersion upon blending with polycarbonate and reduced the electrical percolation from 0.75 to 0.25 wt%.

It should be noted that the key factors governing the preferential localization of typical fillers are thermodynamic, kinetic, and polymer melt viscosity [22]. Thermodynamic considerations state that the filler might reside in one of the polymer phases or at the interface as a result of the overall free energy of the existence of three types of interfaces: polymer 1/polymer 2, filler/polymer 1, and filler/polymer 2. Thermodynamically, the filler location might be predicted from the spreading coefficient parameters [23]. Kinetic effects, on the other hand, are related to the mixing process. An equilibrium state of filler dispersion may not be reached in typical mixing experiments due to high viscosity of the polymers. If the system is quenched before reaching an equilibrium state of filler dispersion, incomplete migration of the filler to the thermodynamically favored phase may result [24]. Another important factor is the melt viscosity of the blend component. It has been reported that the melt viscosity factor promotes the localization of filler in a less viscous phase [21, 22, 24].

The concept of selective localization was used in this study to develop electrically conductive *in situ* composites of LCP in PC. It was hypothesized in view of fibrillar domains of LCP that the selective localization of CNTs in the continuous LCP fibrils would facilitate the anisotropic electrical conductivity in PC/LCP blends and consequently reduce the electrical percolation threshold compared to PC/CNT composites. Continuous fibrils of LCP have been observed previously in blends of polycarbonate [2], polypropylene [25], poly(ether imide) [26], and polyamide 66 [3], with LCP content in the range of 15–35 wt%. Mukherjee et al. [27] recently reported improvements in mechanical properties of PC/LCP blends in the presence of up to 5 wt% carboxylated CNTs and attributed such improvements to compatibilization effects produced by hydrogen bonding interactions between the COOH groups on CNTs and the carbonyl groups in PC and LCP. These authors observed much smaller droplets of LCP phase with the increase of CNT concentration. Although not explicitly stated in their paper, such interactions would be most effective if carboxylated CNTs remained at the PC-LCP interfaces. Electrical conductivity also showed an increase from an insulator at 1 wt% loading of caboxylated CNT to conductive composite with volume electrical conductivity of approximately 5.5×10^{-3} S/cm and 6.5×10^{-3} S/cm, respectively, at 3 wt% and 5 wt% CNT. Bose et al. observed higher percolation threshold in the cocontinuous polyamide 6 (PA6)/acrylonitrile-butadiene-styrene (ABS) blends containing CNTs compared to the ABS/CNT composites [28]. They found that the nanotubes preferentially resided in PA6 as PA6 displayed a closer value in surface energy as well as a lower melt viscosity. The authors explained their results in terms of good wettability of CNTs by insulating PA6 that led to the suppression of electrical conductivities observed in the PA6/ABS/CNT system.

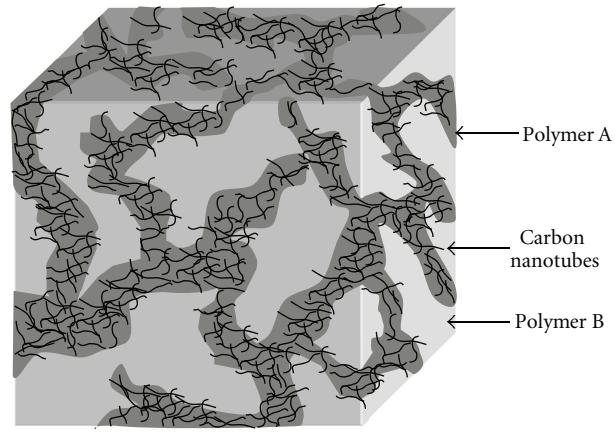

Figure 1: Schematic showing double percolation phenomena for carbon black-containing polymer composites.

In this contribution, PC/LCP blends were produced with 20 wt% LCP and the rheological, morphological, electrical, and mechanical properties of the resultant PC/LCP/CNT composites were characterized. The morphological changes in the blends caused by the introduction of CNTs were related to the changes in viscosity and the consequent reduction of electrical conductivity. Several specific questions were answered in this work, which were not addressed in the work of Mukherjee et al. [27, 29]. First, it was not clear from the outset if unmodified CNTs would remain at the interface, move to either the LCP or PC domains, or distribute both in PC and LCP domains in the blend. The images provided in Mukherjee et al. [27] and taken via a high-resolution transmission electron microscope were inconclusive about the location of CNTs. Specific knowledge of CNT localization

Table 1: Physical properties of the materials used.

Materials	Density (g/cm^3)	Glass transition temperature, T_g (°C)	Melting point, T_m (°C)	Melt flow index (g/10 min)
PC	1.20	149.4	—	18 (300°C/1.2 kg)
V400P	1.40	110	225	14 (230°C/2.16 kg)
VA950	1.40	100	280	Not available from the supplier[a]
CNT	0.13–0.15 (bulk density)	—	—	—

[a]The melt flow index of VA950 cannot be measured under the test conditions as stated by the manufacturer.

in LCP or PC domains would in turn help rationalize the trend of electrical conductivity of the blends. Second, the impact of the feeding sequence on the distribution of CNTs in the PC and LCP phases should be examined. Specifically, CNT was first compounded with LCP and the resultant blend was mixed with PC. In another experiment, CNT was compounded first with PC and then with LCP.

2. Experimental

2.1. Materials. Polycarbonate was supplied by SABIC Innovative Plastics (Mt Vernon, IN) as Lexan 121. Two grades of LCPs—VA950 and V400P were obtained from Ticona (Florence, KY). The multiwalled carbon nanotube was obtained in the form of Baytubes, C-150P of approximate diameter 13 nm and length > 1 μm from Bayer MaterialScience (Pittsburgh, PA). A selection of properties of these components is listed in Table 1.

2.2. Composite Preparation. Compounds were prepared in a twin-screw, minicompounder (HAAKE MiniLab) at 290°C for neat PC and PC/V400P/CNT, and at 300°C for PC/VA950/CNT, with a rotational speed of 60 rpm. All the components were dried in a vacuum oven at 120°C for 8 hrs. The feeding sequence was as follows: PC and CNT were melt-mixed in a minicompounder for 5 minutes, taken out, then melt-mixed again for 5 minutes with the addition of a certain amount of an LCP. Samples with the prefix "REV" are of the reversed mixing sequence, where CNT was first mixed with LCP followed by mixing the compound with PC. The composite compositions were kept the same in both sequences.

Injection-molded samples were prepared using a mini-injection-molding machine from DSM research with the injection-molding temperature and mold temperature of, respectively, 310°C and 150°C for PC, V400P and PC/V400P/CNT, and 300°C and 80°C for VA950 and PC/VA950/CNT. The injection pressure was $6 \times 10^5\,kg\,m^{-1}\,s^{-2}$ for all samples. The injection-molded rectangular bars were cut into the dimensions of 36.0 mm × 12.0 mm × 2.0 mm and 30.0 mm × 6.5 mm × 2.0 mm for the determination of electrical conductivity and dynamic mechanical properties, respectively. The discs of PC, V400P, and VA950 with 28 mm diameter and 0.8 mm thickness were used in measurements of contact angle.

3. Characterization

The rheological properties of the samples were investigated using ARES (TA Instruments) rotational rheometer. The frequency sweep measurement was performed with 25 mm parallel plate geometry, in oscillatory shear mode, and a fixed strain amplitude of 2%. A Rame-Hart contact angle goniometer (Model 100-00) operating at 1 atm and a temperature of 24 ± 2°C was used for measurement of contact angle of two reference liquids, di-iodomethane and deionized water. A Keithley sub-Femtoamp Remote SourceMeter four-point conductivity probe (model 6430) was used for measurement of electrical conductivity of the compounds with a current of 10 μA for low resistivity samples and a voltage of 100 V for high resistivity samples. The morphology of LCP in PC/LCP/CNT compounds was examined by scanning electron microscopy (SEM, JEOL SM-71510) and transmission electron microscopy (TEM, Tecnai 12 TEM). For this purpose, PC was dissolved by immersing the blends in chloroform at room temperature for 12 h and the LCP residue was recovered by filtration. Therefore, all SEM images presented in this paper show only the LCP phase. The dynamic mechanical analyzer (RSA III) was used to study the mechanical response, such as storage modulus and loss modulus of the samples at temperature ranging from 35°C to 200°C and a heating rate of 4°C/min. These tests were conducted in single point bending mode with a fixed strain of 0.2% and a vibration frequency of 1 Hz.

4. Results and Discussion

4.1. Melt Rheology. The melt rheological response in frequency sweep was recorded at two temperatures according to the injection molding conditions, that is, 300°C for the systems comprising of VA950, and at 310°C for those comprising of V400P. As evident in Figures 2(a) and 2(b), at both temperatures, the PC showed Newtonian behavior and both LCPs exhibited non-Newtonian behavior, that is, the complex viscosity ($|\eta^*|$) decreased with increasing frequency. It is widely accepted that fibril formation of the LCP in a thermoplastic matrix is governed by two major factors—the ratio of viscosity of LCP and the matrix polymer and the value of interfacial tension between the polymer components. The LCP with lower viscosity than the matrix polymer tends to deform into fibrils. In other words, the viscosity ratio of less than unity is promising for fibrillation of the LCP phase. In addition, sufficiently low interfacial tension between LCP and the matrix polymer is also required for good fibril formation. Also, the LCP content must be high to yield substantially large LCP domains, which in turn would facilitate elongation of the LCP domains. It was found that the values of $|\eta^*|$ of VA950 at 300°C were slightly

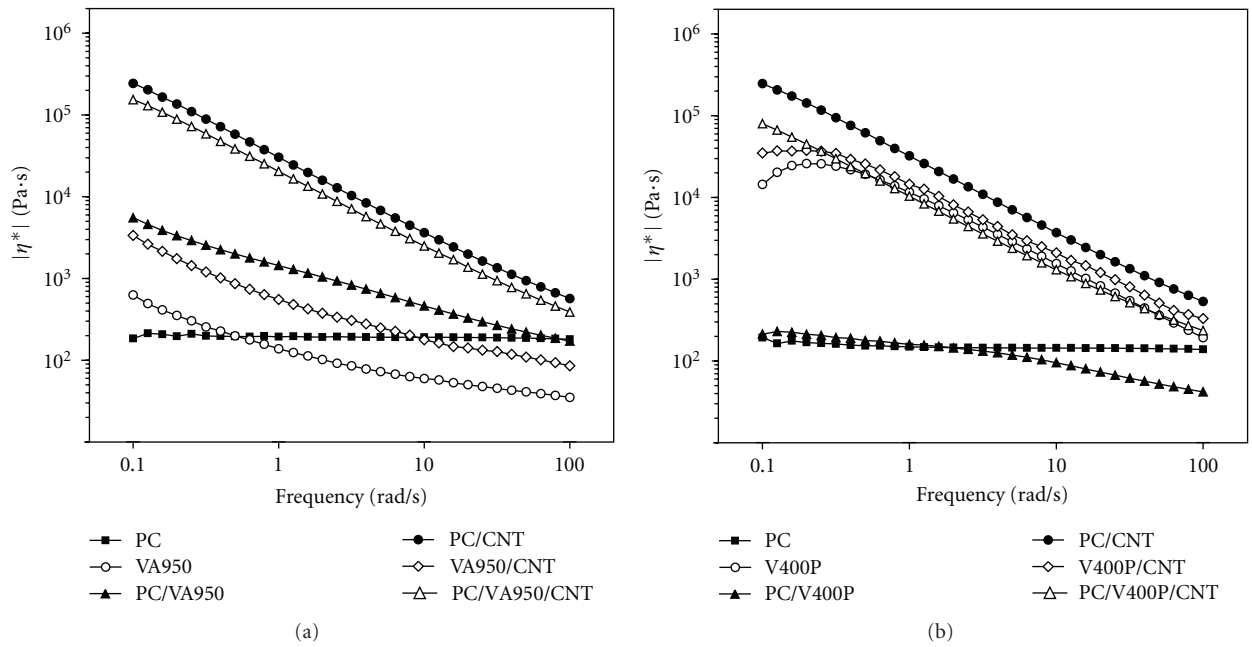

Figure 2: Comparison of complex viscosity for PC, PC/LCP blends, and composites with 5 wt% CNT. (a) V400P, measured at 310°C, (b) VA950, measured at 300°C.

greater than those of PC at very low frequencies (from 0.1 to 0.8 rad/s), and lesser at higher frequencies (from 0.8 to 100 rad/s), indicating that the viscosity ratio of VA950 and PC was less than unity during injection molding. The blend of PC with 20 wt% VA950 showed viscosity higher than the individual polymer components. This can be attributed possibly to trans-esterification at the interfaces of PC and VA950 as observed by Tovar et al. [30]. It is also not surprising that the viscosity increased in compounds with the addition of CNTs. The viscosity of PC/VA950 with 5 wt% CNT was slightly lower than PC with 5 wt% CNT and was greater than VA950 with 5 wt% CNT. At 310°C, V400P exhibited the upward concavity at low frequency (Figure 2(b)) which is often found in LCP. The V400P grade of LCP also showed higher viscosity than PC and, therefore, was expected to form spheres instead of fibrils in PC. As expected, the viscosity of this LCP also increased in the presence of CNTs. The viscosity of PC/V400P with 5 wt% CNT was found to be lower than the composites of the corresponding polymer components containing 5 wt% CNT. This can be attributed to the lubricating effect of the V400P domains brought about by immiscibility between a flexible coil-like polymer such as polycarbonate and a rigid-rod LCP as supported by arguments from statistical thermodynamics [31].

4.2. Calculation of Spreading Coefficient. The two-liquid geometric model was used to calculate the surface energy (1) [32, 33] of the polymeric solids with the aid of contact angle measurements:

$$\gamma_{LV}(1+\cos\theta) = 2\left(\gamma_S^d\gamma_{LV}^d\right)^{1/2} + 2\left(\gamma_S^p\gamma_{LV}^p\right)^{1/2}. \quad (1)$$

In (1), γ_{LV} and γ_S are the surface energies of the reference liquid and the polymer, respectively, the superscript d refers to the dispersion part and p refers to the polar part, and θ is the measured contact angle. It should be noted that the surface energy is the sum of the dispersion and the polar parts:

$$\gamma = \gamma^d + \gamma^p. \quad (2)$$

The interfacial energies (γ_{12}) can be calculated from the surface energies using two widely used methods—the geometric-mean equation (3) and the harmonic-mean equation (4) [34]:

$$\gamma_{12} = \gamma_1 + \gamma_2 - 2\left(\sqrt{\gamma_1^d\gamma_2^d} + \sqrt{\gamma_1^p\gamma_2^p}\right), \quad (3)$$

$$\gamma_{12} = \gamma_1 + \gamma_2 - 4\left(\frac{\gamma_1^d\gamma_2^d}{\gamma_1^d+\gamma_2^d} + \frac{\gamma_1^p\gamma_2^p}{\gamma_1^p+\gamma_2^p}\right). \quad (4)$$

In (3) and (4), γ_i stands for the surface energy of the component i ($i = 1, 2$), γ_i^d and γ_i^p are the dispersive part and the polar part, respectively. A fairly successful approach to predict the morphology of the blends with a matrix component and two dispersed components was proposed by Harkins [35]. The Harkins equation predicts the tendency of a liquid to spontaneously spread across the solid or liquid substrate using interfacial tension data. It was proposed in a three component system that component 3 encapsulates component 1 if the spreading coefficient λ_{31} given in (5) is positive:

$$\lambda_{31} = \gamma_{12} - \gamma_{32} - \gamma_{13}. \quad (5)$$

In (5), the three terms on the right are the interfacial energies between the respective components. Table 2 shows

Table 2: Contact angle of polymers at 25°C.

Material	Contact angle (degree)	
	Diiodomethane	Water
PC	29.2	72.2
V400P	25.3	60.0
VA950	29.9	70.0

Table 3: Surface energies (in mJ/m^2) based on the two-liquid geometric method.

Material	γ^d	γ^P	γ	Polarity (%)
PC	39.36	6.50	45.86	14.2
V400P	17.56	24.06	41.62	57.8
VA950	38.42	7.79	46.21	16.9
CNT	18.4	26.9	45.3	59.4

the contact angle values measured with di-iodomethane and water, which were used to calculate the surface energy values reported in Table 3 using γ^d_{LV} and γ^p_{LV} of the reference liquids provided by Kaelble [36]. Although there was some disagreement in literature for the contact angle data for PC [37–39], and VA950 [40, 41], those values still cover our experimental values. The surface energy of V400P has not yet been reported by others and the values for CNT were taken from [42]. The polarity of the materials was found in the following order: CNT > V400P > VA950 > PC. Since the carbonaceous materials tend to localize in more polar polymers [43], we anticipated that CNT would migrate towards the LCP phase. The interfacial energy of PC/VA950 was found to be much lower than that of PC/V400P (see Table 4) suggesting that the former should be a more compatible blend than the latter and, therefore, should be more conducive to fibrillation by LCP. The spreading coefficients of PC/V400P/CNT and PC/VA950/CNT were found to be 0.92 and 1.45 mJ/m^2, respectively, after considering CNT as component 1, PC as component 2, and LCP as component 3, and after substituting the interfacial energy values in Harkins equation. The positive value of λ_{31} indicated that carbon nanotubes would be encapsulated by the LCP domains. It should be noted that the discussion in this paragraph was based on the values of surface tension data obtained at room temperature. In this context, it is recognized that the changes in surface tension of most polymers with respect to temperature were comparable, for example, 0.06–0.08 dyne · cm deg K^{-1} [34, 44, 45].

4.3. Morphology. SEM images of LCP residue extracted from PC/V400P and PC/VA950 blends are presented in Figure 3. The V400P phase in injection molded specimens remained in the form of droplets with the number-average diameter of 0.61 μm and a weight average diameter of 0.67 μm (Figure 3(a)) as a result of lower viscosity of PC. The average diameter was computed from the diameter of at least 100 droplets measured from the SEM images.

The as-compounded PC/VA950 blends taken from the minicompounder also show spherical VA950 domains with number-average diameter of 0.49 μm and a weight-average diameter of 0.60 μm (Figure 3(b)). The VA950 domains in both fibrillar and spherical forms were found in injection molded specimen as in Figure 3(c). This can be attributed to lower pressure generated in the mini-injection molder and low rate of shear in mold filling, typically around 1.0 s^{-1}. One may expect more elongated fibrils in a high speed injection molding process, where the shear rate greater than 10 s^{-1} is typically encountered. First, higher rate of deformation and second, lowering of the viscosity ratio at higher shear rate may cause more extensive fibrillation. Subdued fibrillation and underdeveloped fibrillar structures of LCP domains may also have resulted from the feeding sequence. For example, prior mixing of CNT with LCP increased the viscosity of the LCP phase and hence increased the viscosity ratio of LCP/PC blends. In this case, only spherical domains were obtained as seen in Figure 4. Similar observations were made by Mukherjee et al. [27] in the presence of carboxylated CNTs. The surface of the droplets became rough as a result of the presence of LCP-coated CNT of ~50 nm diameter, although the diameter of as received nanotube was reported to be 13 nm. The mixing sequence was found to influence both the size and the shape of the LCP phase morphology. For example, larger and irregular dispersed VA950 domains were found when CNT was first mixed with VA950 (Figure 4(c)) compared to those of the reversed mixing sequence (Figure 4(b)). In the reversed mixing sequence, CNT increased the viscosity of the PC-phase and accordingly produced much lower viscosity ratio of LCP to PC than in mixtures without CNT.

Figure 5 shows the TEM micrographs of the PC/CNT and PC/LCP/CNT composites. All these samples contained 5 wt% of CNT. The PC/CNT composite shows good CNT dispersion (Figure 5(a)) whereas PC/LCP/CNT composites (Figures 5(b) and 5(c)) clearly reveal nonuniform CNT dispersion. The darker areas present in Figures 5(b) and 5(c) in the form of spheroids are actually the LCP domains. Clearly, the CNTs mainly resided inside the LCP droplets especially in composites of V400P LCP, in agreement with the SEM images seen in Figure 4. Some differences are noticeable in CNT dispersion between the composites PC/VA950/5 wt% CNT and PC/V400P/5 wt% CNT. For example, the TEM image in Figure 5(c) shows that CNT particles were present in both PC-phase and inside LCP domains when VA950 was used, while as per Figure 5(b), CNTs were mostly contained in V400P LCP domains. The interfacial energy data presented in Table 4 shows that CNT had very close affinity for PC and VA950 LCP, with interfacial energy of respectively 10.9 and 9.4 mJ/m^2. On the other hand, CNTs showed more affinity to V400P LCP with interfacial energy of 0.09 mJ/m^2. From the melt viscosity point of view, the filler tends to reside in the less viscous phase. This is in accordance with the localization of CNTs in the VA950 domains. On the other hand, the presence of V400P, having higher viscosity than PC, would result in the suppressed migration of the nanotubes into V400 phase and thus competing with the thermodynamic driving force. According to Persson and Bertilsson, viscosity effects are weak and dominate only when the difference of interactions between the filler/polymer1 and

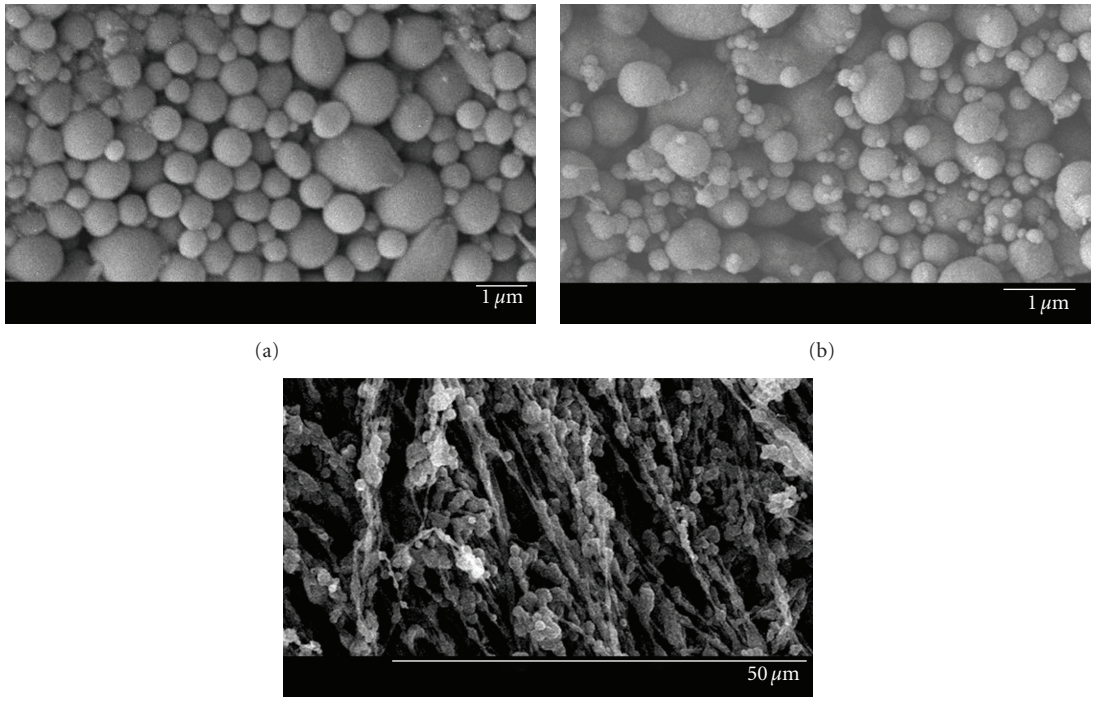

(a) (b)

(c)

Figure 3: SEM micrographs of the LCP residues of PC/V400P (a) injection-molded specimen, (b) as-compounded PC/VA950, and (c) PC/VA950 injection-molded specimen.

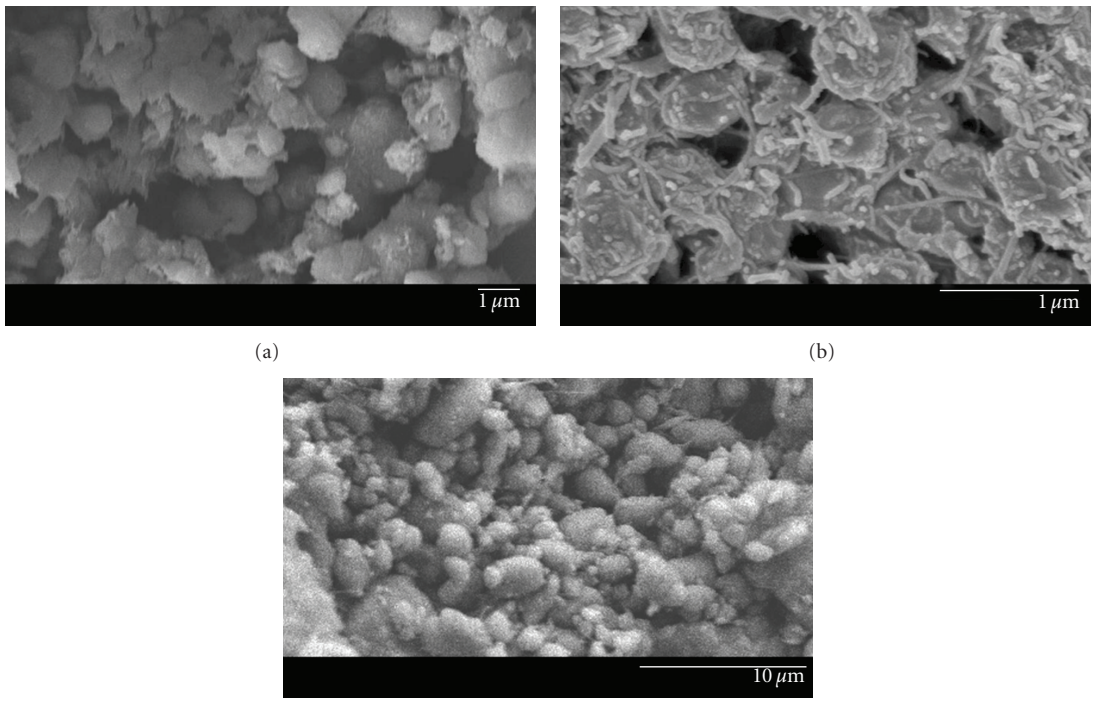

(a) (b)

(c)

Figure 4: SEM micrographs of the LCP residues of injection-molded specimen of (a) PC/V400P/5 wt% CNT, (b) PC/VA950/5 wt% CNT, (c) PC/VA950/5 wt% CNT with reversed feeding sequence.

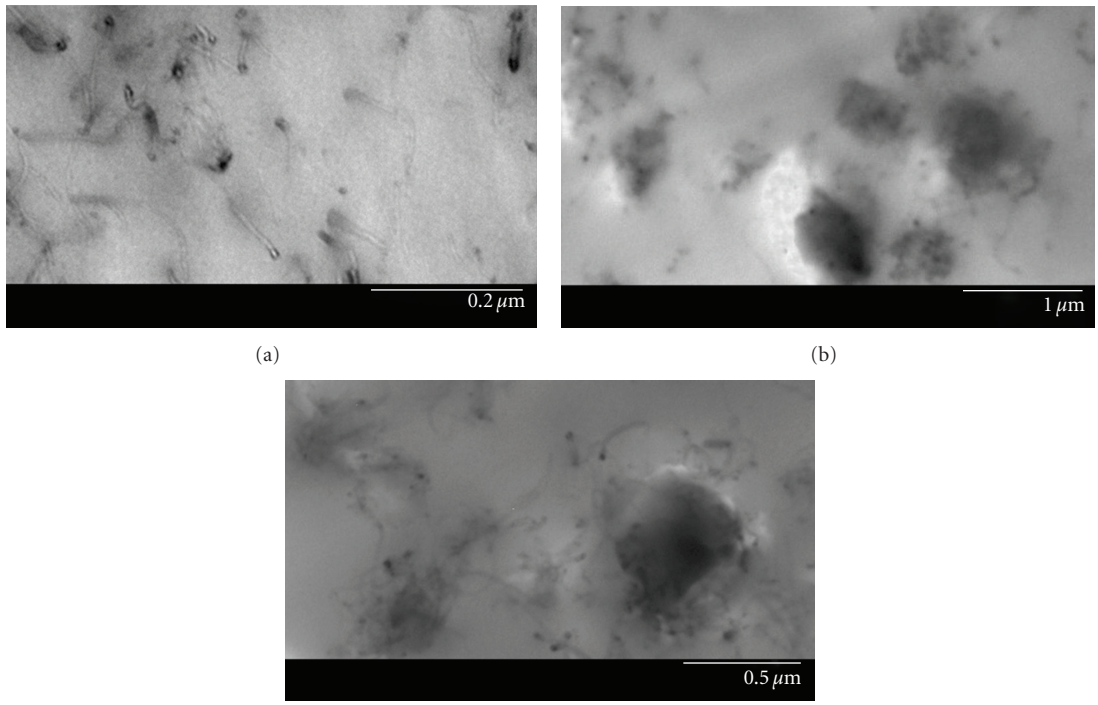

Figure 5: TEM micrographs of the thin sections of composites with 5 wt% CNT based on the (a) neat PC, (b) PC/V400P, and (c) PC/VA950.

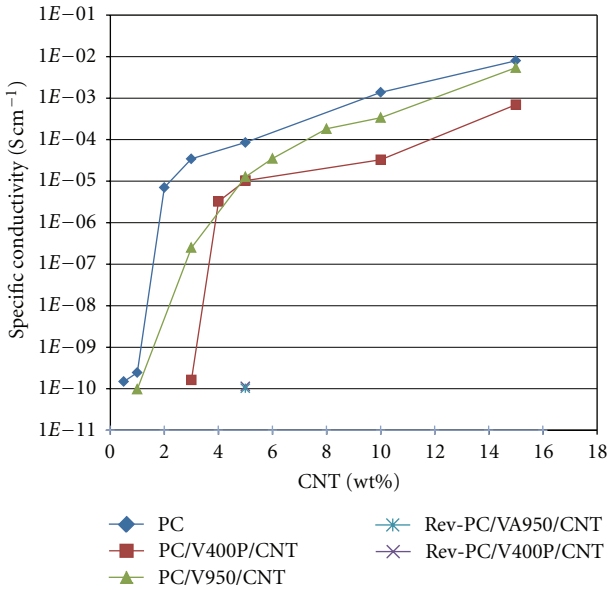

Figure 6: The specific conductivity of composites as function of CNT weight percent.

filler/polymer 2 is small [24, 46]. Since such difference in the PC/V400P/CNT system is quite large, it is not surprising that the thermodynamic factor prevailed on the viscosity factor, that is, the nanotubes selectively localized in V400P domains.

Table 4: Interfacial energies calculated from the geometric-mean equation and the harmonic-mean equation.

Material	Interfacial energy (mJ/m^2)	
	Geometric-mean equation	Harmonic-mean equation
PC/CNT	10.9	20.0
V400P/CNT	0.09	0.18
VA950/CNT	9.4	17.6
PC/V400P	9.9	18.4
PC/VA950	0.06	0.13

4.4. Electrical Conductivity. Figure 6 provides the specific electrical conductivity of five compounds as function of CNT content. The electrical conductivity at 5 wt% CNT can be expressed in the following order with the numbers in parentheses representing electrical percolation threshold: PC/CNT (1 wt%) > PC/VA950P/CNT (1 wt%) > PC/V400P/CNT (3 wt%). In this case, the percolation threshold was taken as the starting point of sharp rise of electrical conductivity. In light of the SEM and TEM images presented in Figures 4 and 5, it can be inferred that the nanotube conductive pathways were destroyed due to subdued fibrillation in the presence of either type of the LCP. The composites of LCP and CNT were found to be insulators even when the CNT content was as high as 10 wt%. Compounds of V400P and VA950 with up to 15 wt% CNT did not produce conductive composites. Therefore, in addition to restricted fibrillation, the increase in the electrical percolation threshold as well as

Table 5: Storage moduli, G′ at 40°C, for PC, PC/ LCP blends, and composites with 5 wt% CNT.

Material	PC	PC/CNT	V400P	V400P/CNT	PC/V400P	PC/V400P/CNT	VA950	VA950/CNT	PC/VA950	PC/VA950/CNT
G′ (GPa)	1.58	1.73	4.30	4.83	2.25	1.57	3.05	4.28	1.74	1.83

the lowered electrical conductivity of the blends may result from encapsulation of the nanotubes with the insulating LCP as predicted by thermodynamic factors. Similar observation in blends of ABS/PA6/CNT was reported by Bose et al. [28].

Nevertheless, the composite of PC/VA950P/CNT showed percolation at 1 wt% CNT loading. This can be attributed to the presence of CNTs on the rough surfaces of VA950/CNT domains as seen in Figure 4(b) and corroborated by TEM image presented in Figure 5(c). A distinct shift in the percolation threshold to the higher CNT loading was observed in composites of V400P LCP. Although the melt viscosity of V400P was significantly higher than that of the PC matrix, the good affinity between this LCP and the nanotubes rendered the confinement of a large number of CNTs within the V400P phase. Consequently, only a small amount of CNT was available to span the matrix or to bridge across the LCP domains to form an electrical percolation network. For blends of PC/VA950/CNT, the spreading coefficient also predicts the migration of CNTs to the better-wetting VA950 phase, but not to the same extent as the blend with V400P. Subsequently, the formation of the electrical network by CNTs was more favored in the blend containing VA950 as compared to the one with V400P. Overall, the strong insulating properties of an LCP and the tendency of CNT to localize in the LCP-phase lowered the values of electrical conductivity when incorporated into the PC/CNT compounds. The affinity of CNT with both LCPs was demonstrated very clearly by the electrical conductivity values of the REV-PC/LCP/CNT composites. Here, CNT was first mixed with the LCP to obtain composite specimens REV-PC/V400P/CNT, and REV-PC/V950/CNT. During the second mixing step with PC, most of CNT remained in the LCP phase indicating that filler migration to the PC matrix was not favored. Consequently, these composites did not show electrical conductivity even at a loading of 5 wt% CNT. These results comply with the SEM image shown in Figure 4(c).

4.5. DMA Results. Table 5 shows the values of storage modulus at 40°C of three groups of sample—the neat polymers (PC, V400P, VA950), the blends of PC with 20 wt% LCP (PC/V400P, PC/VA950) and the composites of either PC or LCP with 5 wt% CNT (PC/CNT, V400P/CNT, VA950/CNT) or both PC/LCP with 5 wt% CNT (PC/V400P/CNT, PC/VA950/CNT). The storage moduli at less than 110°C of compounds containing V400P showed the following order: V400P/CNT > V400P > PC/V400P > PC/CNT > PC, PC/V400P/CNT. The most surprising result is the lower value of storage modulus of PC/V400P/CNT composite in comparison with PC/V400P blend and V400P/CNT composite. It was expected that the addition of CNT to PC/V400P would increase the modulus further in view of the fact that CNT remained primarily in V400P domains and that V400P/CNT composite showed higher modulus than V400P (Table 5). The only possible explanation of this reduction of storage modulus of PC/V400P/CNT composite may be attributed to potential degradation of molecular weight of PC due to longer exposure (10 minutes) to compounding temperature compared to 5 minutes in other materials. However, reduction of PC molecular weight was not verified using chromatographic method. For VA950-containing compounds, the storage moduli at low temperature show the following trend: VA950/CNT > VA950 > PC/VA950/CNT ~ PC/VA950 ~ PC/CNT > PC. Once again, the storage modulus of PC/VA950/CNT composite remained in the neighborhood of PC/VA950 and PC/CNT, possibly due to molecular weight reduction of the PC phase, the latter attributed to longer exposure of PC to high compounding temperature.

5. Conclusions

Two PC/LCPs blends were designed by adjusting the melt viscosity ratio and the shear rate used in processing, such as injection molding to interpret the trends in mechanical properties and electrical conductivity in terms of CNT localization in LCP domains, PC phase, or at the interfaces. The PC/VA950 blend showed fibrillar structures and PC/V400P blend showed spherical LCP domains. Attempt was made to distribute the CNT in both PC/LCP blends and to determine the percolation threshold of CNT for electrical conductivity, although the positive values of the spreading coefficient parameter for CNT particles promoted preferential localization of CNT inside the LCP domains. PC showed surface energy and polarity comparable to VA950 but different from V400P, due to which double percolation was found to occur only for PC/VA950. Accordingly, PC/CNT and PC/VA950/CNT composites showed the same electrical percolation threshold (1 wt%) while PC/V400P/CNT needed 3 wt% CNT to show electrical percolation. Prior addition of CNT to LCP increased the viscosity of LCP phase further, which increased the viscosity ratio to greater than unity and hindered LCP fibril formation.

Acknowledgments

Financial support was provided in part by the Thailand Research Fund through the Royal Golden Jubilee Ph.D. Program and National Center of Excellence for Petroleum, Petrochemicals and Advanced Materials.

References

[1] P. Pisitsak and R. Magaraphan, "Rheological, morphological, thermal, and mechanical properties of blends of vectra A950

and poly(trimethylene terephthalate): a study on a high-viscosity-ratio system," *Polymer Testing*, vol. 28, no. 2, pp. 116–127, 2009.

[2] L. P. Tan, C. Y. Yue, K. C. Tam, Y. C. Lam, and X. Hu, "Effects of shear rate, viscosity ratio and liquid crystalline polymer content on morphological and mechanical properties of polycarbonate and LCP blends," *Polymer International*, vol. 51, no. 5, pp. 398–405, 2002.

[3] H. Wang, K. W. Lee, T. S. Chung, and M. Jaffe, "Rheology, morphology and properties of LCP/nylon 66 composite fibers," *Polymer Composites*, vol. 21, no. 1, pp. 114–123, 2000.

[4] S. Saengsuwan, S. Bualek-Limcharoen, G. R. Mitchell, and R. H. Olley, "Thermotropic liquid crystalline polymer (Rodrun LC5000)/polypropylene in situ composite films: rheology, morphology, molecular orientation and tensile properties," *Polymer*, vol. 44, no. 11, pp. 3407–3415, 2003.

[5] R. Viswanathan and I. A. Isayev, "Blends of a PPO-PS alloy with a liquid crystalline polymer," *Journal of Applied Polymer Science*, vol. 55, no. 7, pp. 1117–1129, 1995.

[6] W. Bu and I. A. Isayev, "Prepregs and laminates of polyetherimide-reinforced by a thermotropic," *Journal of Applied Polymer Science*, vol. 56, no. 2, pp. 329–340, 1997.

[7] I. Isayev and S. Swaminathan, "Wholly aromatic polyester fiber-reinforced polyetherimide composite and process for preparing same," European Patent EP 0 291 323, A2, 1994.

[8] R. Tchoudakov, M. Nakis, and A. Seigmann, "Electrical conductivity of polymer blends containing liquid crystalline polymer and carbon black," *Polymer Engineering & Science*, vol. 44, no. 3, pp. 528–540, 2004.

[9] Y. W. Wong, K. L. Lo, and F. G. Shine, "Electrical and thermal properties of composite of liquid crystalline polymer filled with carbon black," *Journal of Applied Polymer Science*, vol. 82, no. 6, pp. 1549–1555, 2001.

[10] J. Bao, C. Xu, W. Cai, and X. T. Bi, "Electrically conductive composite of polypyrrole and liquid crystalline copoly(ester-amide)s," *Journal of Applied Polymer Science*, vol. 52, no. 10, pp. 1489–1497, 1994.

[11] M. Sumita, K. Sakata, Y. Hayakawa, S. Asai, K. Miyasaka, and M. Tanemura, "Double percolation effect on the electrical conductivity of conductive particles filled polymer blends," *Colloid & Polymer Science*, vol. 270, no. 2, pp. 134–139, 1992.

[12] J. C. Huang, "Carbon black filled conducting polymers and polymer blends," *Advances in Polymer Technology*, vol. 21, no. 4, pp. 299–313, 2002.

[13] I. Mironi-Harpaz and M. Narkis, "Thermo-electric behavior (PTC) of carbon black-containing PVDF/UHMWPE and PVDF/XL-UHMWPE blends," *Polymer Engineering and Science*, vol. 41, no. 2, pp. 205–221, 2001.

[14] R. Tchoudakov, O. Breuer, M. Narkis, and A. Siegmann, "Conductivity/Morphology Relationships in immiscible polymer blends: HIPS/SIS/Carbon black," in *Conductive Polymers and Plastics in Industrial Applications*, L. Rupprecht, Ed., p. 51, William Andrew Publishing/Plastics Design Library, New York, NY, USA, 1999.

[15] D. P. Dharaiya, S. C. Jana, and S. F. Lyuksyutov, "Production of electrically conductive networks in immiscible polymer blends by chaotic mixing," *Polymer Engineering and Science*, vol. 46, no. 1, pp. 19–28, 2006.

[16] C. Zhang, X. S. Yi, H. Yui, S. Asai, and M. Sumita, "Morphology and electrical properties of short carbon fiber-filled polymer blends: high-density polyethylene/ poly (methyl methacrylate)," *Journal of Applied Polymer Science*, vol. 69, no. 9, pp. 1813–1819, 1998.

[17] C. Zhang, P. Wang, C. A. Ma, G. Wu, and M. Sumita, "Temperature and time dependence of conductive network formation: dynamic percolation and percolation time," *Polymer*, vol. 47, no. 1, pp. 466–473, 2006.

[18] P. Pötschke, A. R. Bhattacharyya, and A. Janke, "Carbon nanotube-filled polycarbonate composites produced by melt mixing and their use in blends with polyethylene," *Carbon*, vol. 42, pp. 965–969, 2004.

[19] P. Pötschke, A. R. Bhattacharyya, and A. Janke, "Morphology and electrical resistivity of melt mixed blends of polyethylene and carbon nanotube filled polycarbonate," *Polymer*, vol. 44, no. 26, pp. 8061–8069, 2003.

[20] P. Pötschke, S. Pegel, M. Claes, and D. Bonduel, "A novel strategy to incorporate carbon nanotubes into thermoplastic matrices," *Macromolecular Rapid Communications*, vol. 29, no. 3, pp. 244–251, 2008.

[21] S. Bose and A. R. Bhattacharyya, "Rheology, electrical conductivity and the phase behaviour of cocontinuous PA6/ABS blends with MWNT: correlating the aspect ratio of MWNT with the percolation threshold," *Journal of Polymer Science B*, vol. 46, pp. 1619–1631, 2008.

[22] V. Mittal, Ed., *Specific Interactions Induced Controlled Dispersion of Multiwall Carbon Nanotubes in Co-Continuous Polymer Blends, in Polymer Nanotube Nanocomposites: Synthesis, Properties, and Applications, Chapter 13*, John Wiley & Sons, Hoboken, NJ, US, 2010.

[23] S. Y. Hobbs, M. E. J. Dekkers, and V. H. Watkins, "Effect of interfacial forces on polymer blend morphologies," *Polymer*, vol. 29, no. 9, pp. 1598–1602, 1988.

[24] F. Fenouillot, P. Cassagnau, and J. C. Majesté, "Uneven distribution of nanoparticles in immiscible fluids: morphology development in polymer blends," *Polymer*, vol. 50, no. 6, pp. 1333–1350, 2009.

[25] H. H. Chen, J. P. deSouza, D. G. Baird, K. T. The, and J. Morton, "Processing of in situ composites based on thermoplastic matrices and liquid crystalline polymers," in *Proceedings of the 9th International Conference on Composite Materials (ICCM '93)*, vol. 5, p. 467, July 1993.

[26] A. I. Isayev and S. Swaminathan, "Wholly aromatic polyester fiber-reinforced polyetherimide composite and process for preparing same," U.S. Patent 4,835,047, 1989.

[27] M. Mukherjee, T. Das, R. Rajasekar, S. Bose, S. Kumar, and C. K. Das, "Improvement of the properties of PC/LCP blends in the presence of carbon nanotubes," *Composites A*, vol. 40, no. 8, pp. 1291–1298, 2009.

[28] S. Bose, A. R. Bhattacharyya, A. R. Kulkarni, and P. Pötschke, "Electrical, rheological and morphological studies in co-continuous blends of polyamide 6 and acrylonitrile-butadiene-styrene with multiwall carbon nanotubes prepared by melt blending," *Composites Science and Technology*, vol. 69, no. 3-4, pp. 365–372, 2009.

[29] M. Mukherjee, S. Bose, G. C. Nayak, and C. K. Das, "A study on the properties of PC/LCP/MWCNT with and without compatibilizers," *Journal of Polymer Research*, vol. 17, no. 2, pp. 265–272, 2010.

[30] G. Tovar, P. J. Carreau, and H. P. Schreiber, "Transesterification, morphology and some mechanical properties of thermotropic liquid crystal polymers/polycarbonate blends," *Colloids and Surfaces A*, vol. 161, no. 1, pp. 213–223, 2000.

[31] P. J. Flory, "Statistical thermodynamics of mixtures of rodlike particles. 5. Mixtures with random coils," *Macromolecules*, vol. 11, no. 6, pp. 1138–1141, 1978.

[32] D. K. Owens and R. C. Wednt, "Estimation of the surface free energy of polymers," *Journal of Applied Polymer Science*, vol. 13, no. 8, pp. 1741–1747, 1969.

[33] D. H. Kaelble, "A reinterpretation of organic liquid- polytetrafluoroethylene surface interactions," *Journal of Adhesion*, vol. 2, pp. 50–60, 1970.

[34] S. Wu, *Polymer Interface and Adhesion*, Marcel Dekker, New York, NY, USA, 1982.

[35] W. D. Harkins, *The Physical Chemistry of Surface Films*, Reinhold, New York, Ny, USA, 1952.

[36] D. H. Kaelble, *Physical Chemistry of Adhesion*, Wiley Interscience, New York, NY, USA, 1970.

[37] J. L. Dewez, E. Humbeek, E. Everaet, A. Doren, and P. G. Rouxhet, *Polymer-Solid Interfaces*, Institute of Physics Publishing, Bristol, UK, 1991.

[38] S. Jonsson, *Presented at Aspects of Adhesion*, Radcure, Middlesex, UK, 1992.

[39] J. S. Cho, "Metallized Plastics Surface modification of polymers by ion-assisted reactions: an overview," in *Adhesion Aspects of Thin Films*, K. L. Mittal, Ed., vol. 2, p. 105, VSP, Utrecht, The Netherlands, 2005.

[40] K. X. Ma, T. S. Chung, and R. J. Good, "Surface energy of thermotropic liquid crystalline polyesters and polyesteramide," *Journal of Polymer Science B*, vol. 36, no. 13, pp. 2327–2337, 1998.

[41] T. S. Chung, K. X. Ma, and M. Jaffe, "Experimental and theoretical estimations of surface tensions for commercial liquid crystalline polymers, Vectra A-950, B-950 and Xydar SRT-900," *Macromolecular Chemistry and Physics*, vol. 199, no. 6, pp. 1013–1017, 1998.

[42] S. Nuriel, L. Liu, A. H. Barber, and H. D. Wagner, "Direct measurement of multiwall nanotube surface tension," *Chemical Physics Letters*, vol. 404, no. 4–6, pp. 263–266, 2005.

[43] C. F. Schoff, "Painting problem," in *Coatings of Polymers and Plastics*, R. A. Ryntz and P. V. Yaneff, Eds., p. 227, Marcel Dekker, New York, NY, USA, 2003.

[44] S. Wu, "Calculation of interfacial tension in polymer systems," *Journal of Polymer Science C*, vol. 34, no. 1, pp. 43–19, 1974.

[45] G. L. Gaines, "Surface and interfacial tension of polymer liquids-a review," *Polymer Engineering & Science*, vol. 12, no. 1, pp. 1–11, 1997.

[46] A. L. Persson and H. Bertilsson, "Viscosity difference as distributing factor in selective absorption of aluminium borate whiskers in immiscible polymer blends," *Polymer*, vol. 39, no. 23, pp. 5633–5642, 1998.